*17th World Conference on Earthquake Engineering, 17WCEE*
*Sendai, Japan - September 13th to 18th 2020*

# UNREINFORCED MASONRY WITH THERMAL INSULATION FACADES IN MULTI-STORY BUILDINGS SUBJECTED TO SEISMIC TYPE LOADS

G.C. Manos[1)], L. Melidis[2)], K. Katakalos[3)], V. Soulis[4)], A. Anastasiadis[5)]

[(1)] *Professor Emeritus, Lab. Strength of Materials and Structures, Aristotle University, Thessaloniki, Greece, gcmanos@civil.auth.gr*
[(2)] *Post. Student, Lab. Strength of Materials and Structures, Aristotle University, Thessaloniki, Greece, lazmelidis@gmail.com*
[(3)] *Asst. Professor, Lab. Strength of Materials and Structures, Aristotle University, Thessaloniki, Greece, kkatakal@civil.auth.gr*
[(4)] *Dr. Civil Engineer, Lab. Strength of Materials and Str., Aristotle University, Thessaloniki, Greece, vassilios_soulis@yahoo.com*
[(5)] *Dr. Civil Engineer, Research Associate, Thessaloniki, Greece, anastasiadis@asacon.eu*

## *Abstract*

Unreinforced masonry panels within multi-story reinforced concrete (R/C) or steel framed structures were damaged to a considerable extend during past strong earthquake activity. The realism of numerically simulating the cyclic earthquake-type behaviour of masonry infilled R/C frames was studied extensively by comparing numerical predictions with results from a series of pseudo-dynamic tests on masonry infilled R/C frame specimens. An advanced non-linear 2-D numerical simulation was validated which can realistically capture the in-plane hysteretic behaviour of reinforced concrete (R/C) frames with masonry infills when subjected to combined in-plane vertical and cyclic seismic-type horizontal load. The present work is another step in investigating the earthquake performance of unreinforced masonry panels when a thermal insulation jackets are attached on the external façades of these masonry panels. A number of such unreinforced brick masonry panels with or without thermal insulation attachments are built and tested subjecting them to either in-plane or out-of-plane forces. The tested specimens employed thermal insulation attachments produced by a Greek industry emploung fixtures and thermal insulation materials and techniques that are utilized in prototype building structures. These unreinforced brick masonry panels are first subjected to in-plane axial compression. Next, they are subjected to out-of-plane flexural forces. Finally, they are firmly supported on a the strong reaction frame and floor of the Laboratory of Strength of Materials and Structures of Aristotle University subjected to a combination of in-plane and out-of-plane loads aiming to replicate the state of stress that develops in such a masonry panels when the whole multi-story structural formation is subjected to prototype earthquake excitations. Results of this experimental sequence are presented and discussed in an effort to record the interaction between the brick masonry and the thermal insulation attachment and the relevant modes of failures. It was observed, through the limited testing executed up to now, that the in-plane and the out-of-plane flexural bearing capacity of the specimens including the used thermo-insulation, is larger than the corresponding bearing capacity of similar specimens without the used thermo-insulating attachments. The observed limit state for the specimens with thermo-insulation was partial debonding of the insulating panel. The used plastic anchors prevent, up to a point, the complete debonding of such thermo-insulating panels. 3-D finite element simulation of the out-of-plane flexural behaviour was formed utilizing commercial software. In these numerical simulations all the geometrical, loading and support details of tested specimens were numerically simulated. Such numerical simulations included non-linear interfaces in an effort to numerically simulate the observed behaviour. In this way, the observed response was successfully captured by these numerical simulations. The methodology adopted here includes testing samples of the materials used to verify their basic mechanical properties and sub-assemblies of masonry wallets with insulating panels subjected to out-of-plane loading, combined with numerical models developed, and it is considered, up to a point, satisfactory. This methodology will be further validated with additional experimental results and parametric investigation in a variety of specimen geometry and materials used.

*Keywords: masonry infills, thermal insulation, multi-story building, seismic load, measured and numerical response*

*Dedicated to the memory of the late Professor Hiroshi Akiyama of the University of Tokyo and the late Professor Heki Shibata of the Institute of Industrial Science, University of Tokyo.*

## 1. Introduction

Unreinforced masonry panels are used in multi-story buildings made of steel or reinforced concrete (R/C) to form the exterior facades or the interior partitions. Thermo-insulating panels are also attached on the exterior facades of these masonry panels in order to improve the energy efficiency of these building as well as to reduce noise and moisture penetration. This type of masonry façades is widely applied in many countries. These unreinforced masonry panels are considered as non-structural elements not included in the structural design. Such un-reinforced masonry panels interact with the surrounding structural members, when such structures are subjected to strong earthquake motions. This is because these masonry panels are forced to follow the displacement response of the supporting surrounding structural members (slabs, columns and beams) leading to potentially damaging conditions. The resulting damaging patterns for these masonry panels bear re-semblance, up to a point, to bearing masonry structural elements when they are subjected to earthquake type forces. Thus, it is helpful to distinguish dam-age due to either in-plane or out-of-plane seismic forces. One of the most serious consequence of either of these forcing scenarios, when the seismic forces are considered as acting either separately (in-plane or out-of-plane) or combined, is the dislocation and partial collapse of such un-reinforced masonry panels. Figure 1 depicts a typical damage pattern observed in numerous mutli-story buildings in Durres, Alba-nia due to the recent strong earthquake sequence (26th November, 2019). Similar damage patterns have been observed in many past strong earthquake sequences in Greece (Kozani 1995, Aigio 1995, Athens 1999, Kefalonia 2014) as well as in many other countries (Italy, L' Aquila 2009, Emilia Romana 2012) [1, 2].

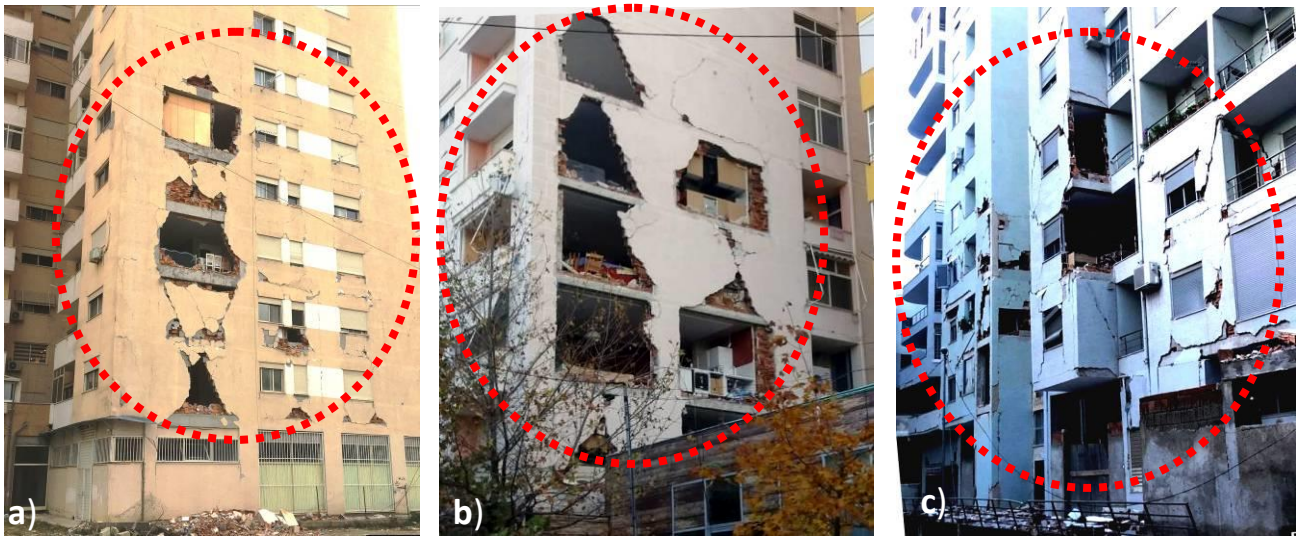


Fig. 1. Collapse of unreinforced masonry facades of multi-story R/C buildings at Durres, Albania (2019).

Thus, the seismic vulnerability of un-reinforced masonry panels has been demonstrated by numerous prototype earthquakes in many countries. At this point, one can distinguish two types of masonry panels. The first type is a masonry panel that is confined within the bay formed by two columns and as the one depicted in figures 2a and 2b. Such a bay is called masonry "infilled" frame and it has been the subject of extensive research for some-time [ ]. The second type, depicted in figure 1a,b,c and 2c . This time the masonry panels are either not built within a bay formed by structural members, as described before, or are partially built and as such they have very limited confinement. Therefore, their progressive damage can easily lead to partial collapse. The necessity to deal with the impact of strong earthquake on masonry infilled R/C frames by relevant seismic design provisions has been long recognized. This is done by relatively such new updated seismic design provisions like the ones included in Euro-Code 8 (1996), American FEMA-306 (1999) and the newest Greek Structural Intervention Regulation (2009). These provisions are based on several methodologies which have been proposed in the past to take into account the influence of masonry infills on



 

the overall behavior of masonry infilled R/C frames when they are subjected to horizontal seismic loads. However, the performance of the infill walls and the attached components should be further investigated, as the possible economic losses and casualties due to collapsed walls cannot be ignored. An additional feature that must be considered, when examining the vulnerability of un-reinforced masonry panels subjected to seismic forces, is the incorporation of thermo-insulating materials. This is shown in figures 3a and 3b whereby double wythe masonry panels are constructed leaving a cavity in between whereby a layer of thermo-insulating material is placed. As shown by figures 3a and 3b, such a construction practice increases the vulnerability of a masonry panel when subjected to seismic forces.


Fig. 2. Collapse of unreinforced masonry facades of multi-story R/C buildings in L'Aquila, Italy (2009).

Based on the above observations, it is essential to study the performance of masonry panels incorporating thermo-insulating layers, when these masonry panels are subjected to forces that produce within these panels stress-fields resembling those that are resulting from seismic actions. This is the objective of an ongoing research at Aristotle University which aims to investigate both the in plane and the out of plane behavior of masonry panel specimens together with External Thermal Insulating Systems (ETICs). The thermo-insulating materials are produced by "FIBRAN Anastasiadis Dimitrios S.A." and are applied on the specimens to be tested in the same way that are applied in prototype construction, as will be explained in the following. The specimens are ma-sonry sub-assemblies which are constructed and tested at the Laboratory of Strength of Materials and Structures (Aristotle University of Thessaloniki, Greece), as discussed in sections 2 and 3. In section 4, summary results from a number of numerical simulations are presented. These numerical simulations were performed aiming to numerically replicate the observed response of the masonry sub-assembly specimens during testing. All the informa-tion of the geometry and material characteristics of mortar, bricks and ETICs material specimens used in building these masonry assemblies were utilized during these numerical simulations.

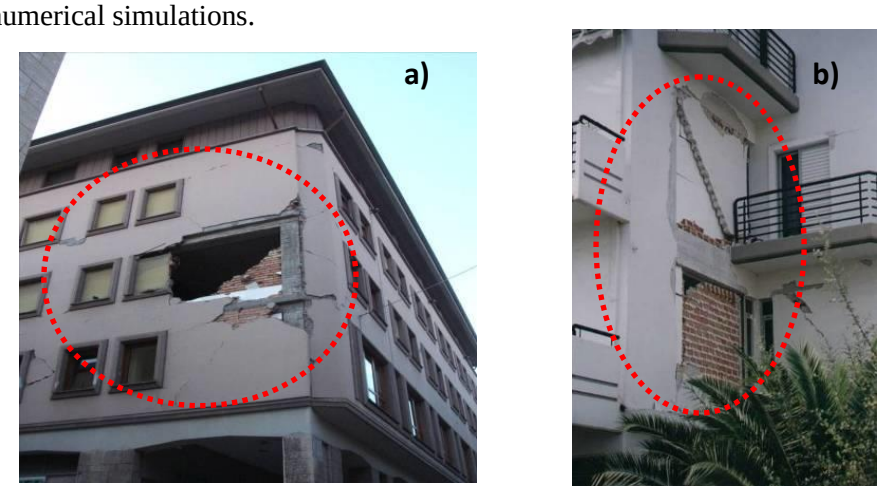


Fig. 3. Collapse of double wythe brick masonry facade with thermo-insulation layer in its cavity a) L'Aquila, Italy, 2009 earthquake, b) Athens, Greece, 1995 Earthquake.



 

## 2. Experimental program

All specimens were built with the same 12 hole clay brick unit of nominal dimensions length=320mm, height=180mm and thickness=150mm, having a mean gross compressive strength equal to 2.95MPa [4, 6]; this brick unit is commonly used in prototype construction for this type of un-reinforced masonry panels in multi-story buildings in Greece. Similarly, a relative weak mortar, with an average cubic strength equal to 2.42MPa was used for all specimens. The thermo-insulating layer was added to one side of all specimens two months following their construction, as shown in figure 4, following the relevant construction practice. Three different thermo-insulating materials, with code names XPS, EPS and Petro, were investigated, having a panel thickness of either 50mm or 100mm, all produced by "FIBRAN Anastasiadis Dimitrios S.A." All specimens were built by builders following the relevant prototype work conditions. Specimens of all materials used for building these specimens were taken during construction and tested for determining the relevant mechanical characteristics. Due to space limitations they are not reported here.

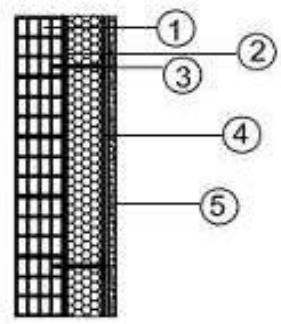


1. Masonry wall
2. Adhesive mortar interface used to attaching the thermo-insulating panel to the masonry façade
3. Plastic anchors also used to attaching the thermo-insulating panel to the masonry facade
4. Thin mortar layer protecting the thermo-insulating panel
5. Thin plastic reinforcing net that is attached with special thin mortar layer to form the final surface

Fig, 4. Construction detail of the masonry specimens with the thermo-insulating attachment.

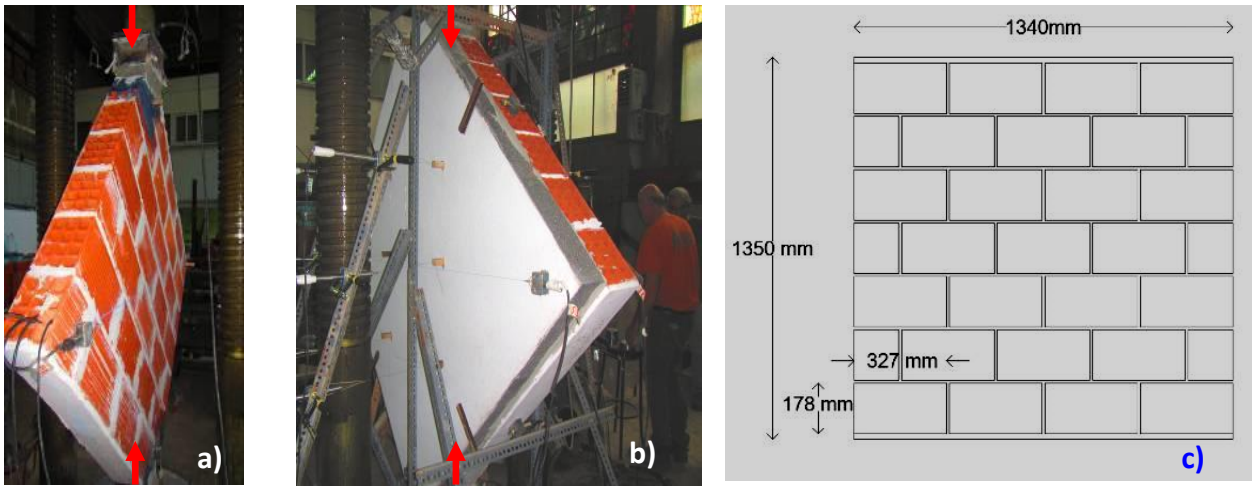


Figure 5. Diagonal in-plane compression of unreinforced brick masonry wallets. a) without b) with thermo-insulating façade. c) Typical dimensions of the specimens (nominal thickness 150mm)

Initially, specimens of rather medium size, named "wallets", were built and tested in order to investigate the behaviour of the thermo-insulating panel attached on the masonry when subjected to specific relatively simple loading conditions. For these wallets, one loading condition was designed to subject a specimen, with an almost square shape, to a compressive force (in-plane) along its main diagonal, as shown in figures 5a, and 5b, thus resulting in a mainly in-plane state of stress. Figure 5c depicts the basic dimensions of such specimens. A second loading condition was designed to subject a wallet , with a rectangular shape (length 2000mm, height 970mm and thickness 150mm), to an out-of-plane forcing, as depicted in figure 6a. This wallet was placed on a supporting steel frame having its upper and lower horizontal sides simply-supported,



 

whereas the vertical sides were completely free. The out of plane load was introduced through an electronically controlled servo-actuator, as shown in figure 6a, thus subjecting this wallet to out-of-plane flexure. Figure 6a depicts the thermo-insulating façade of one wallet specimen together with the instrumentation aimed to capture the out-of-plane displacement response. Figures 6b and 6d depict the basic dimensions of this type of wallets together with certain details of the employed thermo-insulating scheme.

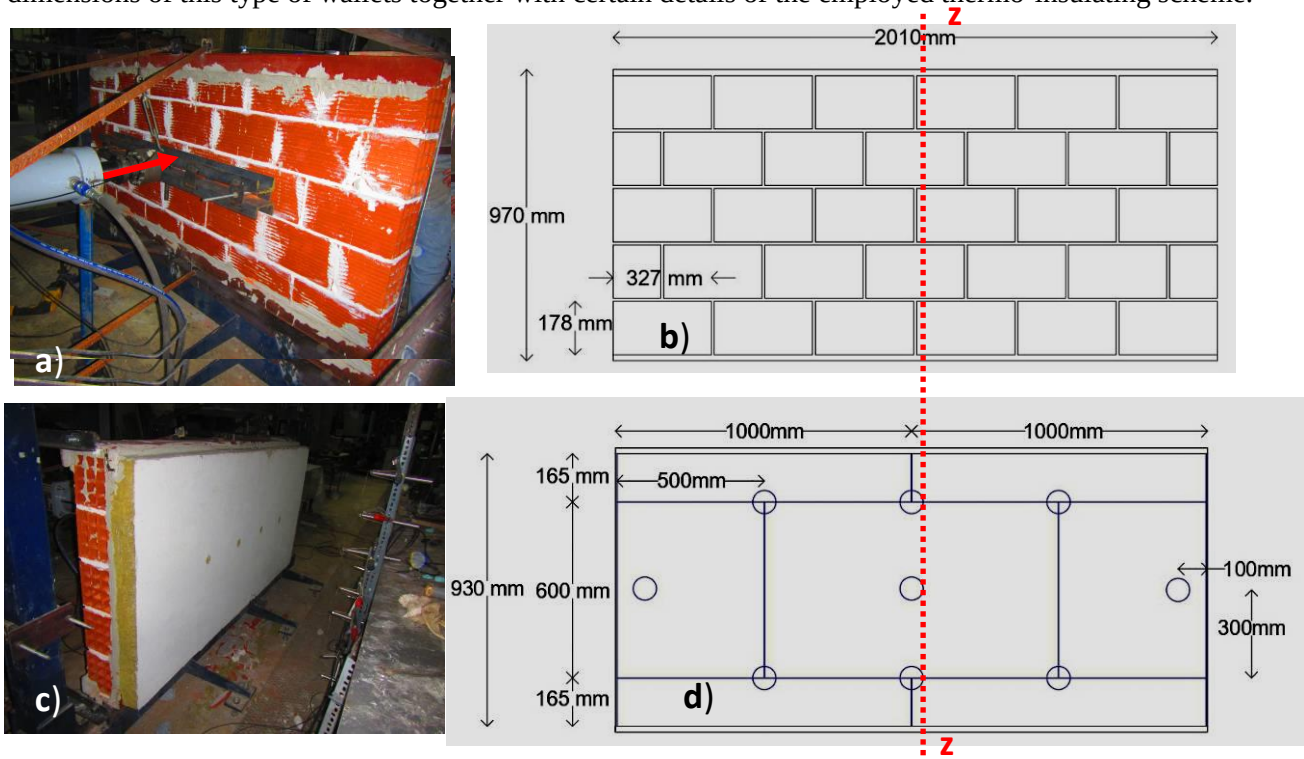


Fig. 6. Out-of-plane flexure of a masonry wallets. a) and b) View from the brick façade. c) and d) View from the thermo-insulating (mineral wool) façade. The circles indicate the location of the anchors.

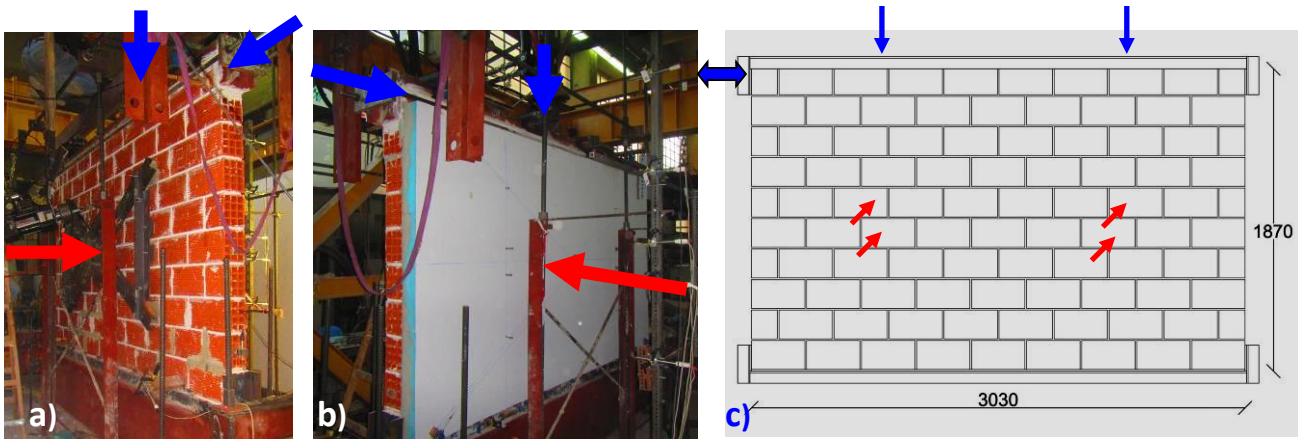


Fig. 7. Combined in-plane and out-of-plane loading of a masonry walls. a) View from the brick façade. b) View from the thermo-insulating façade. c) Basic dimensions of wall specimens (nominal thickness 150mm).

Next, specimens of relatively larger dimensions than the wallets, named “walls” were also built. These wall specimens were built with the same bricks, mortar and thermo-insulating materials that were used for the wallets. They were placed in a strong reaction with the capability of applying in-plane and out-of-plane combined loading as is indicated in figures 7a, 7b and 7c. In this combined loading, the vertical load was



 

kept constant where the applied horizontal in-plane and out-of-plane load were varied in continously incresing cyclic manner, simulating in this way a state of stress resulting from a seimic loading.

## 3. Laboratory measurements

İn what follows a summary of the obtained in-plane and out of plane response of the wallet specimens will be first presented and discussed.. Next, selective preliminary results obtained from testing the wall specimens will also be presented. During all the tests instrumentation was provided to capture the displacemet response in real time. For this purpose, a considerable number of displacement transucers were deployed during each tests. Moreover, the applied in-plane and out-of-plane loads were also con-currently measured.

### 3.1 In-plane diagonal compression

A wallet specimen without any therom-insulation was initially tested. The observed damage was in the form of a diagonal crack along the main vertical diagonal as is shown in figures 8a and 8b. The measured response of this specimen, in terms of shear stress versus shear strain is depicted in figure 9a.

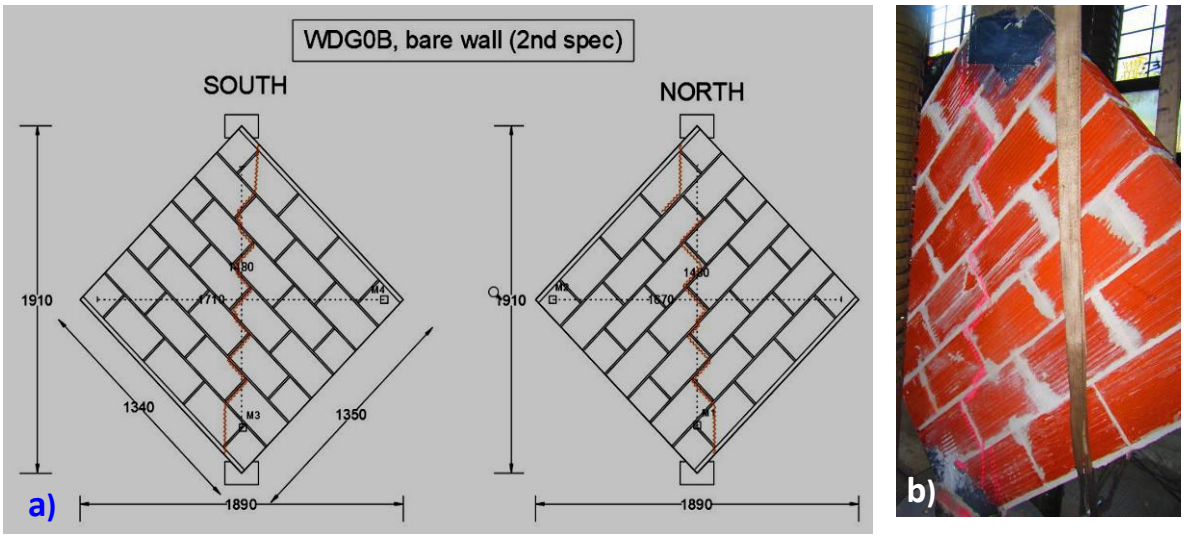


Fig. 8. Observed damage for a wallet without thermo-insulation subjected to diagonal compression.

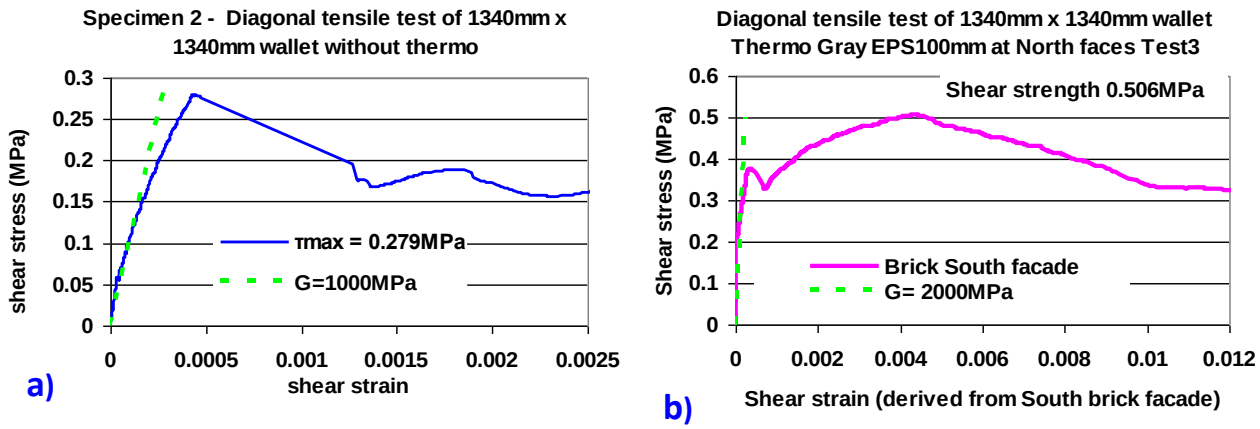


Fig. 9. Measured shear stress versus shear strain response from diagonal compression. a) Wallet without any thermo-insulation. b) Wallet with a thermo-insulating façade constructed with Gray-EPS 100mm thick panel.

Next, a specimen with a thermo-insulating façade was tested under similar diagonal compression conditions. The maximum shear strength that was derived for this specimen is also indicated in this figure together with the corresponding value of the shear modulus. The thermo-insulating attachment in this case is indicated



 

with the code name of the thermo-insulating material (Gray-EPS with a thickness of 100mm). The measured response of this specimen, in terms of shear stress versus shear strain is depicted in figure 9b.

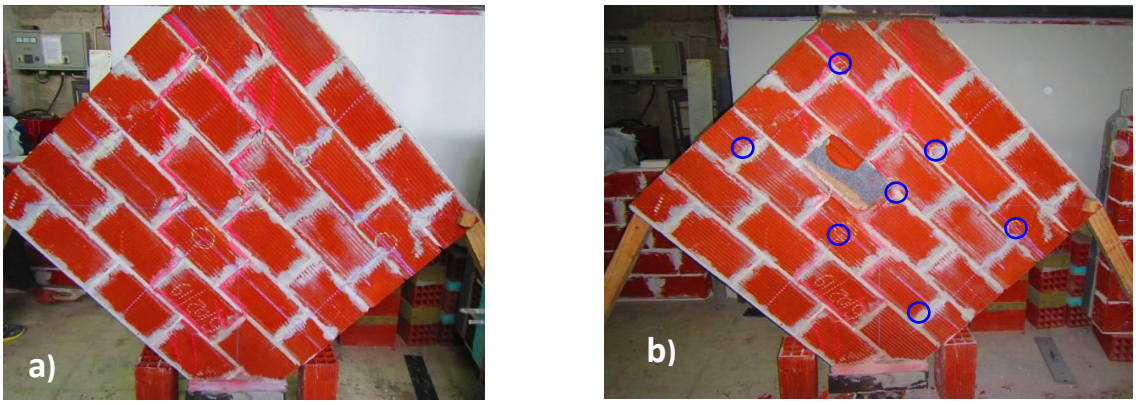


Fig. 10. Observed damage from diagonal compression of wallet with a thermo-insulating façade constructed with Gray-EPS 100mm thick panel. a) View of brick façade with diagonal cracking b) View of brick façade with diagonal cracking and removal of broken brick.

Figure 10 depicts the observed damage from diagonal compression of wallet with a thermo-insulating façade constructed with Gray-EPS 100mm thick panel. In figure 10b the back side of the thermo-insulating panel is also visible after the removal of the broken brick in this region. Moreover, the location of the used anchors is also indicated in this figure. There was no evidence of any debonding of the thermo-insulating panel at this final stage of damage. The rupture of the brick at the central region exposed the central anchor bolt at this location thus rendering it partially ineffective. As can be seen by comparing the shear stress versus shear strain response from diagonal compression in figures 9a and 9b between the wallet without and with thermo-insulating panel the influence of attaching this particular thermo-insulation on the diagonal compression response can be identified. Thus, this attachment resulted in a considerable increase of the measured shear strength as obtained from such a diagonal compression test. Moreover, a considerable increase could also be observed at the amplitudes of the shear strain corresponding to this increased shear strength value.

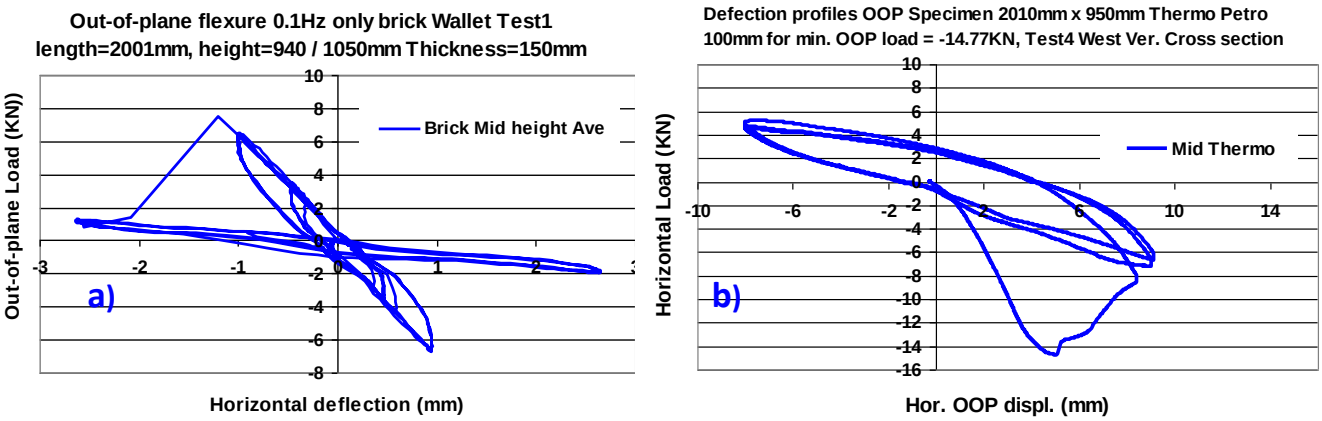


Fig. 11. Measured out-of-plane flexural response of brick wallets. a) Wallet without any thermo-insulation. b) Wallet with a thermo-insulating façade constructed with 100mm thick panel of mineral wool.

## 3.2.Out-of-plane flexural behaviour

In this sub-section the measured out-of-plane flexural behaviour of two wallets is presented. The first wallet is without any thermo-insulation (figure 6a) whereas the second wallet has a mineral wool thermo-insulating attachment with a thickness of 100mm (figure 6c). The dimensions of both wallets are depicted in figures 6b and 6d. The out-of-plane load was applied at a horizontal cross-section located at the mid-height of this wallet (figure 6a). The measured response, in terms of the applied out-of-plane load versus the



 

corresponding out-of-plane displacement at the mid-height central point of the wallet is depicted in figures 11a and 11b. As can be seen in these figures, the presence of this particular thermo-insulating attachment results in a considerable increase of the maximum flexural capacity of the wallet and the corresponding value of the out-of-plane displacement at the middle. When the demand in flexural out-of-plane displacement is further increased it results in extensive cracking of the horizontal mortar joints accompanied by a considerable increase in the out-of-plane displacement response and a sudden reduction of the corresponding out-of-plane load. This is also depicted in figures 12a, 12b and 12c.

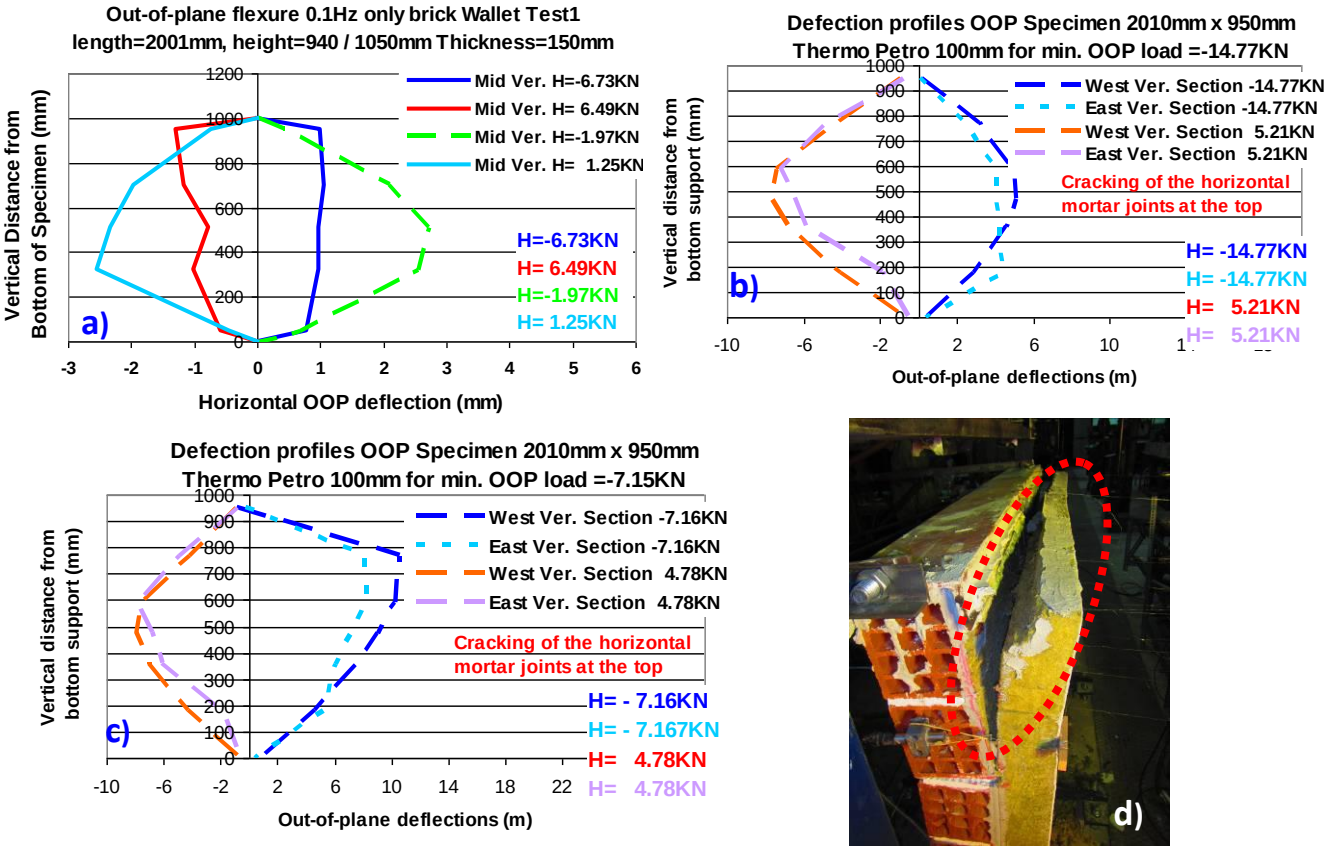


Fig. 12. Observed out-of-plane flexural response of brick wallets. a) Wallet without any thermo-insulation. b) and c) Wallet with a thermo-insulating façade constructed with 100mm thick panel of mineral wool. d) De-bonding of the thermo-insulating panel from the brick wallet at the top part of the wallet.

In these figures, the measured out-of-plane displacement response is plotted for vertical cross-sections (z-z) going through the height of theses wallets (see figures 6a and 6b). Instrumentation was provided in order to capture this out-of-plane displacement response in a number of such vertical cross sections. In figure 12a this out-of-plane displacement response, corresponding to a vertical cross-section going through the central mid-point of the wallet without any thermo-insulating attachment is plotted. The ordinates (y-y axis) in these plot represents the distance of the various points of this vertical cross section from the bottom section of this wallet whereas the abscissae in these plots represent the values of the measured out-of-plane displacements. The various curves plotted correspond to the measured displacement response at various time instants of the loading sequence. For each plotted curve the value of the corresponding measured out-of-plane load is also noted. As can be seen in figure 12a, an increase in the out-of-plane displacement demand larger than approximately 1mm results in a sudden decrease in the out-of-plane bearing capacity for the brick wallet without any thermo-insulating attachment. The presence of the thermo-insulating attachment of mineral wool increases substantially the out-of-plane flexural capacity when the wallet is displaced in a way resulting to the extension of the façade with the thermo-insulating material (figure 12b). In this figure, as well as in figure 12c, the plotted out-of-plane displacement response corresponds to two vertical cross-sections (East



 

and West) located approximately 400mm to the left and right of the central vertical axis of symmetry (z-z figures 6a, 6b) of this wallet. As can be seen this measured displacement response is approximately the same for these two vertical cross-sections. Moreover, as can be seen in figures 12b and 12c, an increase in the out-of-plane displacement demand larger than approximately 5mm results in a sudden decrease in the out-of-plane bearing capacity for the brick wallet with this particular thermo-insulating attachment (see also figure 11b). This large out-of-plane displacement response is accompanied by cracking of the horizontal mortar joints and considerable debonding of the thermo-insulating attachment from the brick wallet (figure 12d).

## 4. Numerical simulations

In what follows numerical models are developed in order to predict the non-linear behavior of clay brick masonry sub-assemblies tested at the laboratory. A 3-D finite element simulation was formed utilizing the capabilities of commercial software. These numerical simulations employed all the geometric and mechanical characteristics of the tested specimen obtained by material testing. The numerical simulations adopt a simplified micro-modeling approach, as the clay bricks are simulated as elastic blocks with linear elastic properties, while the non linear behavior of the specimen is deployed with interfaces between the blocks assigned with non linear stress strain laws. In that way both the failure of the mortar joint and the bonding between a brick and the mortar joint is simulated by the nonlinear interface.

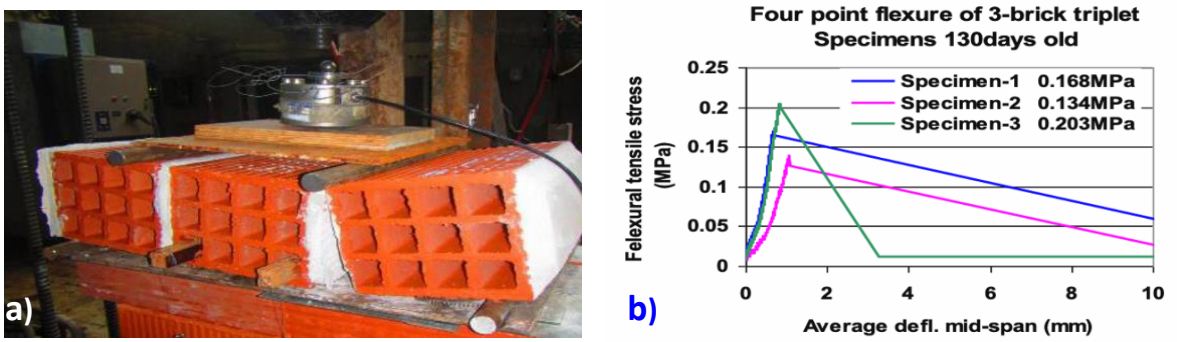


Fig. 13. a) Experimental set up of out of plane triplet bending test b) Flexural stress versus the out of plane displacement obtained by triplet bending tests

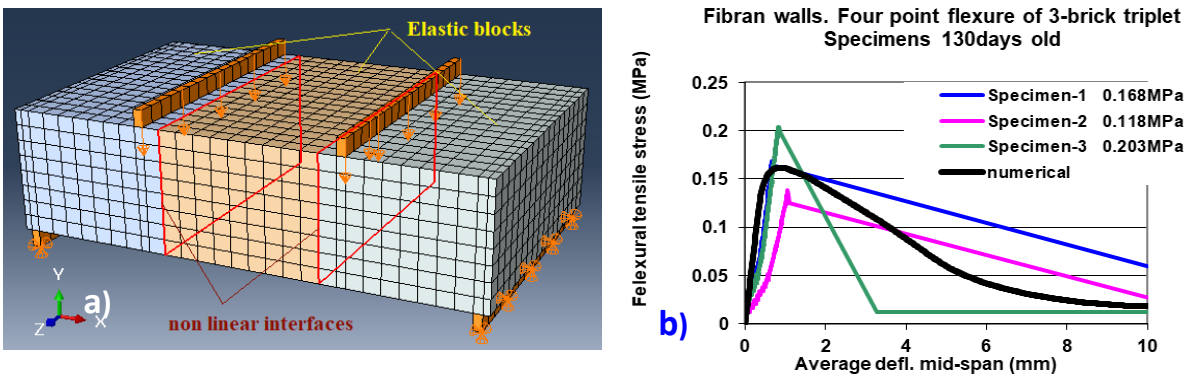


Fig. 14. Numerical simulation of the triplet bending test. a) The numerical model. b) Figure 19: comparison of measured and predicted behavior in terms of flexural stress versus the vertical mid-span deflection for the triplet tests (see figures 13a and 13b)

### 3.3.Out-of-plane flexural behaviour

Prior to testing the brick wallets in flexural out-of-plane load simple flexural tests were performed utilizing triplets specimens made of three clay bricks and two bed mortar joints constructed with the same materials as



 

the wallets presented in section 3. These simple specimens were supported and loaded in a way as to subjected the two mortar joints in pure out-of-plane flexure. This is depicted in figure 13a whereby a triplet specimen is supported at its two ends and loaded in the middle in a typical four-point-bending test. The failing of the right hand side mortar joint is visible in this figure. The obtained results in terms of flexural stress versus the out of plane displacement are shown in figure 13b.

The numerical simulation of the flexural triplet test is formed with the methodology previously described. The geometry, the boundary conditions and the properties assigned are depicted in figure 14a (see also figure 13a). The measured response is compared with the numerical predictions in figure 14b. Figure 15 depicts the distribution of the axial stresses normal to the vertical mortar joints at the step when the maximum load is reached As can be seen, the measured response was successfully captured by the numerical predictions, obtained as described. In what follows, the numerical simulations, developed to predict the response of the wallet specimens with and without any insulating panel, are presented.

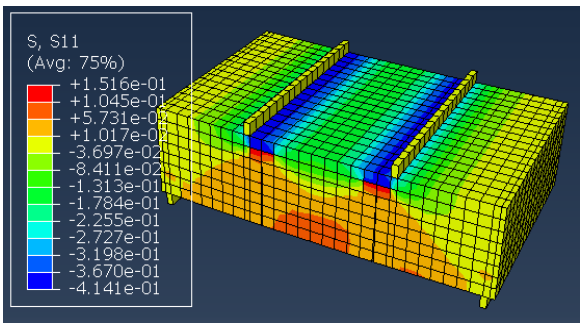


Fig. 15: distribution of the axial stresses normal to the vertical mortar joints at the step when the ultimate load

The numerical methodology described before is again applied for the wallets tested in out-of-plane loads without and with thermo insulation (section 3.2). The insulating panel is represented by solid elements with linear elastic properties attached to the masonry substrate with a 5mm layer of adhesive mortar. The adhesive mortar is also numerically simulated with solid elements assigned with non linear properties, using the "Concrete Damaged Plasticity" constitutive law included in the used commercial software [12], with parameters derived from material testing in compression and four-point flexure. The adhesive mortar and the masonry are connected with a non-linear interface having a tensile strength normal to the wallets plane equal to 0.1MPa. The numerical out-of-plane response of the specimen without thermo-insulation is depicted in figures 16a and 16b (see also figures 12a and 12b). The maximum axial flexural stress is about 0.20MPa almost equal to the maximum one recorded at the experimental sequence described before (figures 13 and 14). Figure 17a and 17b depicts the out-of-plane displacement response of the wallet with 100mm thermo-insulating attachment (see figures 12c and 12d).

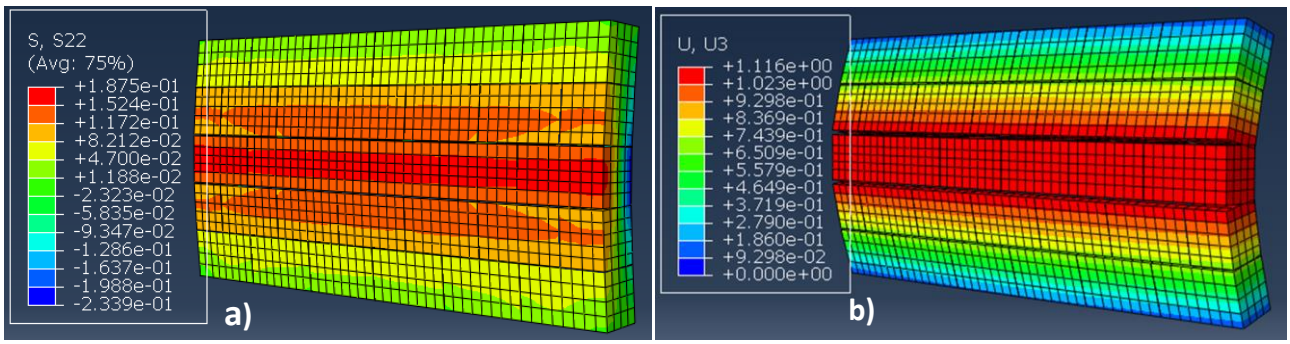


Fig. 16. Numerical simulation of the flexural behaviour of a wallet without thermo-insulation. a) distribution of normal to the joints stresses (MPa) at the step of the ultimate load, bare wallet. b) Predicted mode of failure of the wallet without thermo insulation. U3 displacement (mm) is the out of plane displacement.

As can be seen in figure 17a, at the ultimate state the numerically predicted deformation pattern is that of detachment of the thermo-insulation panel from the masonry, which is quite similar to the observed behaviour (see figure 12d). The comparison of the relevant numerical out-of-plane flexural response of the brick masonry wallets without and with thermo-insulation (100mm mineral wool) is shown in figure 18. In this figure the applied out-of-plane horizontal load is plotted versus the out-of-plane horizontal displacement



 

measured at the center of the wallet. The measured response is compared in this figure with the corresponding numerical predictions. As can be seen the measured maximum load values are in good agreement with the corresponding predictions for both the wallets without and with thermo insulation.

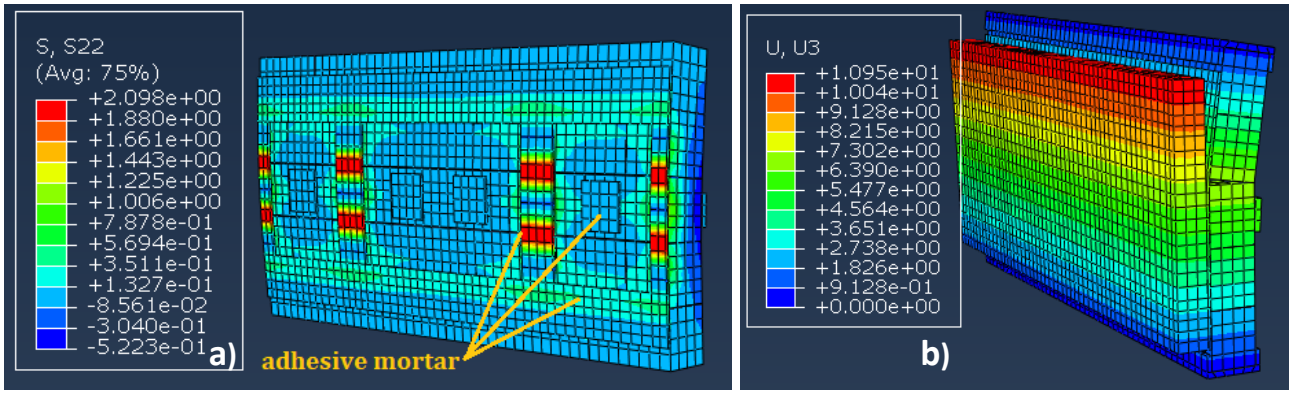


Fig. 17. Numerical simulation of the flexural behaviour of a wallet with 100mm mineral wool thermo-insulation. a) distribution of normal to the joints stresses (MPa) at the step of the ultimate load. b) Predicted mode of failure of the wallet with thermo insulation. U3 displacement (mm) is the out of plane displacement.

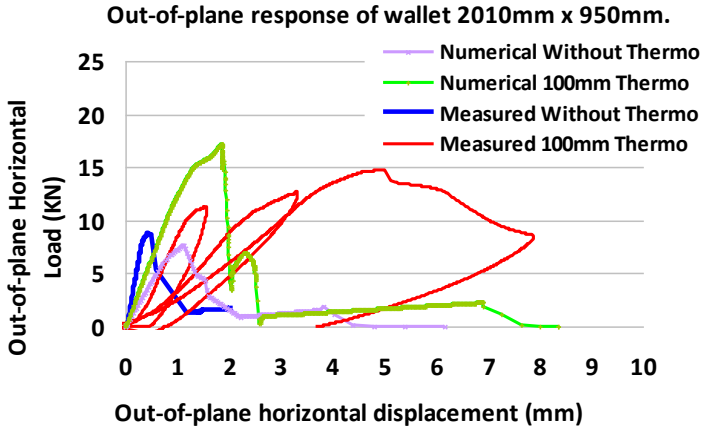


Fig. 18. Out-of-plane response of brick masonry wallets without and with thermo-insulating attachments

## 5. Conclusions

- The current research effort focuses to approximate with simple tests the seismic response of un-reinforced masonry panels, which form the exterior facades or interior partitions of multi-story buildings. Such un-reinforced masonry panels interact with the surrounding structural members, when such structures are subjected to strong earthquake motions, leading many times to considerable damage even collapse of such panels. The focus of the present research effort is to study at the laboratory the performance of masonry assemblies incorporating thermo-insulating layers, when they are subjected to forces producing stress-fields resembling those that are resulting from seismic actions.

- Summary results from the observed in-plane and out-of-plane behavior of masonry wallets constructed with prototype materials, with or without thermo-insulation (EPS, XPS, Mineral Wool), are presented and discussed. It was observed, through the limited testing executed up to now, that the in-plane and the out-of-plane flexural bearing capacity of the specimens including the used thermo-insulation, is larger than the corresponding bearing capacity of similar specimens without the used thermo-insulating attachments. The observed limit state for the specimens with thermo-insulation was partial debonding of the insulating panel. The used plastic anchors prevent, up to a point, the complete debonding of such thermo-insulating panels.



 

- 3-D finite element simulation of the out-of-plane flexural behaviour was formed utilizing commercial software. In these numerical simulations all the geometrical, loading and support details of tested specimens were numerically simulated. Such numerical simulations included non-linear interfaces in an effort to numerically simulate the observed behaviour. In this way, the observed response was successfully captured by these numerical simulations. The methodology adopted here includes testing samples of the materials used to verify their basic mechanical properties and sub-assemblies of masonry wallets with insulating panels subjected to out-of-plane loading, combined with numerical models developed, and it is considered, up to a point, satisfactory. This methodology will be further validated with additional experimental results and parametric investigation in a variety of specimen geometry and materials used.

## 6. Acknowledgements

All materials for the construction of the specimens were provided by "FIBRAN Anastasiadis Dimitrios S.A.". Part of the aforementioned research has been co-funded by Greece and European Union through the Operational Program "Erevno – Dimiourgo -Kainotomo" which are gratefully acknowledged.

Co-financed by Greece and the European Union

## 7. References

[1] Manos G, "Consequences on the urban environment in Greece related to the recent intense earth-quake activity", Int. Journal of Civil Engineering and Architecture, Dec. 2011, Volume 5, No. 12 (Serial No. 49), pp. 1065–1090.

[2] GEER - EERI - ATC - Cephalonia GREECE Earthquake Reconnaissance January 26th/ February 2nd 2014 Version 1: June 6 2014.

[3] Provisions of Greek Seismic Code 2000 , EPPO, Earthquake Planning and Protection Organization Athens, Greece, December 1999.

[4] Euro-Code 6, (2005), "Design of masonry structures - Part 1-1: General rules for reinforced and un-reinforced masonry structures".

[5] FEMA-306 (1999). Evaluation of Earthquake damaged concrete and masonry wall buildings – Ba-sic Procedures manual. Federal Emergency Management Agency, Washington, D.C.

[6] EUROPEAN STANDARD EN 772-1, (2011), "Methods of test for masonry units - Part 1: Determination of compressive strength, May 2011

[7] Euro-Code 8: Design of structures for earthquake resistance - Part 1: General rules, seismic actions and rules for buildings, EN 1998-1, December 2003.

[8] Manos GC, Soulis V, Thauampteh J, "The behavior of masonry assemblages and masonry-infilled R/C frames subjected to combined vertical and cyclic horizontal seismic-type loading" I. J. Advances in Engineering Software 45 (2012) 213–231.

[9] Manos GC, Soulis V, Thauampteh J, "A nonlinear numerical model and its utilization in simulating the in-plane behaviour of multi-story R/C frames with masonry infills", The Open Construction and Build-ing Technology Journal, 2012, 6, (Suppl 1-M16) 254-277.

[10] Manos GC and Soulis V, "Simulation of the in-plane seismic behaviour of masonry infills within Multistory Reinforced Concrete Framed Structures", Proc. 9th Int. Masonry Conference, July, 2014.

[11] Manos GC, Pitilakis KD, Sextos AG, Kourtides V, Soulis V, Thauampteh J, "Field experiments for monitoring the dynamic soil-structure-foundation response of model structures at a Test Site" Journal of Structural Engineering, American Society of Civil Engineers, Special Issue "Field Testing of Bridges and Buildings, D4014012, Vol. 141, Issue 1, January 2015.

[12] Abaqus Unified FEA - SIMULIA™ by Dassault Systèmes.



 